

**RERTR 2012 – 34th INTERNATIONAL MEETING ON
REDUCED ENRICHMENT FOR RESEARCH AND TEST REACTORS**

**October 14-17, 2012
Warsaw Marriott Hotel
Warsaw, Poland**

**Comparative Analysis of Structural Changes in U-Mo Dispersed Fuel
of Full-size Fuel Elements and Mini-rods Irradiated in the MIR Reactor**

A.L. Izhutov, V.V. Iakovlev, A.E. Novoselov, V.A. Starkov,
A.A. Sheldyakov, V.Yu. Shishin, V. M. Kosenkov
RIAR, 433510, Dimitrovgrad-10, Ulyanovsk Region – Russia

and

I.V. Dobrikova, A.V. Vatulin, V.B. Suprun, G.V. Kulakov
VNIINM, P. O. Box 369, 123060, Moscow – Russia

ABSTRACT

The paper summarizes the test and PIE results for low-enriched U-Mo fuel irradiated in the MIR reactor under the RERTR Program. The PIE results were analyzed for both full-size fuel rods and mini-rods containing dispersed fuel in the Al matrix as well as with additions of 2%, 5% and 13% of silicon and protective ZrN coating on the fuel particles. The full-size fuel rods were irradiated up to the average U-235 burnup of ~ 60%; the mini-rods were irradiated up to the average U-235 burnup of ~ 85%. The results show a significant increase of the void fraction in the U-Mo alloy as the U-235 burnup rises from ~ 40% up to ~ 85%. The effect of irradiation conditions and U-235 burnup were estimated with regard to the formation of an interaction layer between the matrix and fuel particles as well as generation of porosity in the U-Mo alloy. The U fission product distribution is shown to change as the U-235 burnup increases from ~ 40% up to ~ 85%.

1. Introduction

About of 70 mini-rods with different characteristics of the U-Mo particles dispersed in the pure Al matrix and second batch ~70 mini-rods contain different amount of silicon in the Al matrix and protective coating on the U-Mo granules have been tested in the MIR reactor. About 520 fuel rods were tested as a part of full-size fuel assemblies. Results of the examination of the IL formation in dispersed full-size fuel assemblies based on tubular fuel elements of the IRT-M type, fuel assemblies of the IRT-U type based on fuel rods and mini-rods with modified dispersed fuel with 5% and 13% Si content in the matrix and protective coatings in the form of an oxidized layer and ZrN on fuel particles that were tested up to the average U-235 burnup of ~ 60% and ~ 85% were presented at the RERTR-2009 [1] and RERTR-2010 [2]. It was shown that in case of 13% Si content in the matrix, the interaction of the U-Mo alloy and the aluminum matrix is practically suppressed up to a burnup of 85%, the fission rate was $\sim 2.3 \times 10^{14} \text{cm}^{-3} \text{s}^{-1}$. It was also noted that

the intensity of the IL generation was higher at higher fission rates even for the 13% Si matrix, the fission rate was $\sim 3.6 \times 10^{14} \text{cm}^{-3} \text{s}^{-1}$. The 2-3 μm thick ZrN protective coating on the U-Mo particles protects them from the interaction with Al matrix. Thus, real way to solve one of the challenges of the dispersed U-Mo fuel, i.e. the interaction of fuel particles with aluminum matrix, were tested. As the fuel burnup increases, this interaction diminish the fraction of Al matrix and the physical and mechanical characteristics of the fuel meat change greatly. In particular, thermal conductivity decreases significantly and the fuel temperature rises. In addition, the matrix plasticity becomes lower and, probably, its resistance to rupture under the fuel particles swelling becomes lower as well. At rather high burnups, fuel particles in the rods undergo deformation because of creep; particles coalescence and when they lose their spherical shape the deformation of the plate-type fuel goes perpendicular to the plate surfaces [3]. The paper presents the analysis of the examination results on the gaseous porosity generation and structural changes of U-Mo particles in full-size IRT-U fuel rods, mini-rods with modified dispersed fuel and in those with pure Al matrix [4]. The X-ray examination results are presented for unirradiated and irradiated fuel composition.

2. Rods basic characteristics and irradiation conditions

Mini-rods with different U-Mo modifications were irradiated from 2003 to 2006 (1st batch). Mini-rods with silicon additions in the matrix and protective coatings on fuel particles were irradiated from 2008 to 2010 (2nd batch) . The full-size fuel rods were irradiated from 2007 to 2009. The basic characteristics of the rods and conditions of their irradiation are presented in Tab1.

Tab. 1: Rods basic characteristics and irradiation conditions.

Parameter	1 st batch of mini-rods	2 nd batch of mini-rods		IRT-U № 19YH 0012006	IRT-U № 19YH 0022006
Fuel	U-9.4 %Mo, U-7.5 %Mo α -phase and (α + γ)-phases	U-9.4 %Mo	U-9.4 %Mo	U-9.4 %Mo	U-9.4 %Mo
U-Mo particles type/size, μm	Granules ~ 100–140 Powder ~ 200–263	Granules ~ 100–140	Granules ~ 100–140	Granules ~ 100–140	Granules ~ 100–140
Matrix material	Al	Al; Al+2%Si; Al+5%Si; Al+13%Si	Al; Al+2%Si; Al+5%Si; Al+13%Si	Al	Al
U content, g/cm ³	~ 4.5; ~ 6.0	~ 6.0	~ 6.0	~ 6.0	~ 6.0
Clad material	SAV-1	SAV-6, alloy 99	SAV-6, alloy 99	SAV-1	AMg-2
Heat flux density, MW/m ² ; av / max..	0,4-0,6/0.6-0.9	1.04 / 1.69	1.13 / 1.74	0.70/ 1.0	0.40 / 0.95
Clad. outer surface T, °C; av / max.	80 / 110	96 /124	112 /146	86 / 115	70 / 106

Parameter	1 st batch of mini-rods	2 nd batch of mini-rods		IRT-U № 19YH 0012006	IRT-U № 19YH 0022006
235U max. burnup, %	~ 20; ~ 52; ~ 70	93.0	67.5	55,6	60,9
Fission rate, $10^{14} \text{cm}^{-3} \times \text{s}^{-1}$; av / max.	~1.0 / ~3.1	~2.3 / ~4.6	~3.6 / ~6.8	1.3 / 2.6	0.8 / 2.6
Max fiss. density 10^{21}cm^{-3}	~1.3; ~3.4; ~4.5	~6.2	~4.5	~4.0	~4.2
Irradiation time, day	85; 210; 290	285	130	235	453

3. Results of the fuel examination

3.1. SEM and EPMA.

For unirradiated rods of all modifications, there is no IL on the U-Mo surface, including pure Al matrix. As fuel burnup increases, mutual diffusion of the matrix and fuel particles components occurs, including fission products. The intensity of this interaction depends greatly on the irradiation conditions and Si content in the matrix.

As for the 1st batch of mini-rods with U content of 6g/cm^3 , at relatively low fission rates and temperatures, the IL made up $\sim 2 \mu\text{m}$, at a fission density of $\sim 1.3 \times 10^{21} \text{cm}^{-3}$; $\sim (5-7) \mu\text{m}$ at a fission density of $\sim 3.4 \times 10^{21} \text{cm}^{-3}$, and $\sim (6-9) \mu\text{m}$ at a fission density of $4.5 \times 10^{21} \text{cm}^{-3}$ [4]. For 2nd batch of mini-rods with pure Al matrix irradiated at 2 times higher fission rates and higher temperatures, the maximal thickness of the IL achieved $\sim (25-30) \mu\text{m}$. The IL volume fraction, IL thickness and atomic ratio of the matrix material (Al+Si) to the fuel particles (U+Mo) for the 2nd batch of mini-rods are listed in Table 2.

Tab 2: Results of the IL volume fraction and (Al+Si)/(U+Mo) atomic ratio measurements for $\sim (100-140) \mu\text{m}$ U-9.4 %Mo fuel granules.

Matrix	B ~ 60%, $\phi \sim 2.3^{\text{av}}/4.6^{\text{max}} 10^{14} \text{cm}^{-3} \text{s}^{-1}$, irradiation time 130 days			B ~ 85%, $\phi \sim 3.6^{\text{av}}/6.8^{\text{max}} 10^{14} \text{cm}^{-3} \text{s}^{-1}$, irradiation time 285 days		
	IL thickness, μm	IL volumetric fraction, %	Ratio (Al+Si)/(U+Mo)	IL thickness, μm	IL volumetric fraction, %	Al+Si)/(U+Mo)
Si<0.4%	~ (25-30)	~ 40±4	~ (7-9)	~ (25-30)	40±4	-
Al+2%Si	~ (15-30)	~ 40±4	~ (5-6)	~ (2-20)	25±3	-
Al+5%Si	~ (2-30)	~ 25±3	-	~ (2-20)	10±2	~ (5-6)*; ≥ 4,7**
Al+13%Si	~ (2-15)	~ 10±2	-	~ (1-10)	6±1	-
ZrN coat, Si<0.4%	-	~ 6±1	-	-	6±1	-

* (Al+Si)/(U+Mo) atomic ratio in the thick IL with no Si;

** (Al+Si)/(U+Mo) ratio in the narrow IL with ≥ 7 at.% Si.

2% of Si in the matrix suppresses the effect of the IL on the growth at a fission rate of $2.3 \times 10^{14} \text{ cm}^{-3} \text{ s}^{-1}$. At a higher fission rate of $\sim 3.6 \times 10^{14} \text{ cm}^{-3} \text{ s}^{-1}$, 2% Si addition does not affect significantly on the U-Mo alloy and Al interaction. The increase of Si content up to 5% and 13% decreases the volume fraction of the IL significantly.

Under the same irradiation conditions but with Si presence in the matrix, the U-Mo - Al interaction is more affected by the U-235 fission rate increase as well as by higher fuel temperature. Here at a U-235 burnup of $\sim 85\%$, the volume fraction of the IL is significantly less as compared to the $\sim 60\%$ burnup. It should be mentioned that mini-rods contained Si additions in the Al matrix had non-uniform in thickness IL and a large scattering (fig 1) in its values (Tab 2). Therefore, to evaluate the intensity of the interaction of fuel particles and matrix, a ratio of the measured area of the IL to the total area of the fuel in the cross-section was used.

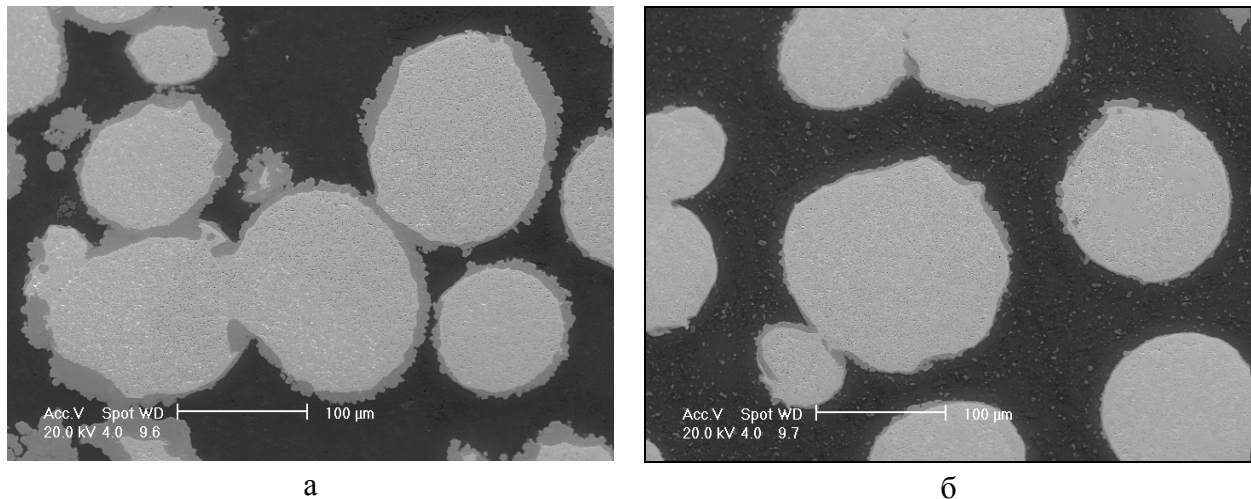


Fig. 1. SEM-images of the fuel (a) - 5% Si, burnup $\sim 85\%$; (b)-13% Si, burnup $\sim 85\%$.

The non-uniform thickness of the IL in the Si alloyed matrix is caused by the non-uniform distribution of Si in the matrix. Another important factor affecting greatly on the generation of IL is a Si-saturated layer on the fuel particle surfaces appeared during the mini-rods manufacturing. Detailed results of the examination of the Si distribution in the mini-rods fuel meat with different Si content and its effect on the IL growth was presented in Ref.[2].

Examinations of the fuel meat structure in the full-size fuel rods showed that U-Mo particles interact with the Al matrix. The layer structure is homogeneous and its width is uniform along the perimeter of the fuel particles, not exceeding $12 \mu\text{m}$ for the fuel elements of both IRT-U type assemblies. The uniform width of the IL in these fuel elements is conditioned by the absence of Si additions in the matrix. The volumetric fraction of the IL in the fuel meat of both assemblies makes up 10 – 12%.

Data on the structure and composition of the IL are also important to describe the U-Mo fuel behavior. That is why a large scope of out-of-pile and post-irradiation examinations was done on this issue. EPMA was used to determine the composition and elements distribution in the fuel meat. Fig 2 presents the EPMA results for the fuel fragment with pure Al matrix at $\sim 60\%$ burnup.

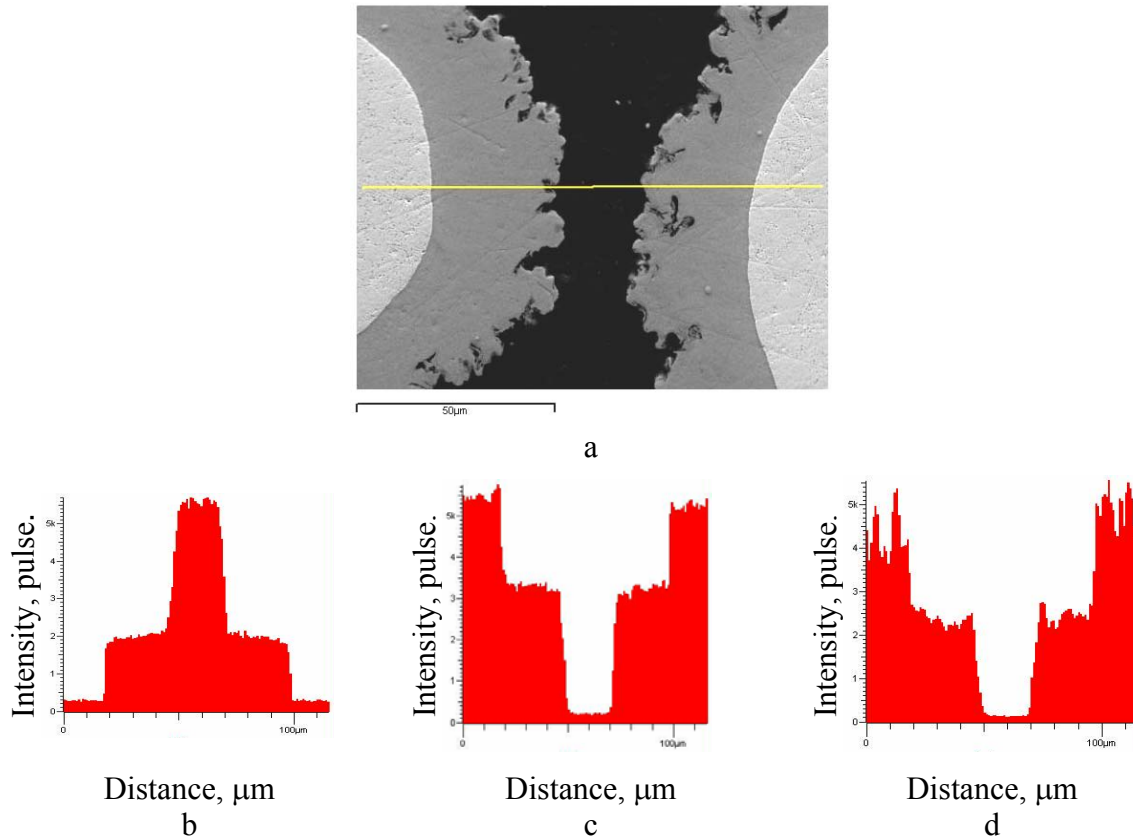


Fig. 2. A section of the fuel (a). Light line shows the electron probe scanning direction: (b) – Al, (c) – U, (d) – Mo.

It should be mentioned that such picture of the Al, Mo and U distribution in the fuel is typical for different fuel burnups and Si content. In all examined cases, the Al and U distribution is rather uniform; an insignificant decrease of the U concentration is observed in the direction from a fuel particle and some decrease of Al concentration is observed in the direction to the fuel particle. Also, it should be mentioned that both optic and electron microscopy did not reveal any differences in the IL structure over its thickness. To evaluate the $(Al+Si)/(U+Mo)$ atomic ratio in the IL of the mini-rods with Al matrix ($Si < 0.4\%$) as well as with 2% and 5% Si content, a quantitative micro-analysis was performed. The results showed this ratio to be different for pure Al matrix and matrix with Si additions. As for Al matrix, the Al/(U+Mo) ratio made up from 7 to 9. These values change in the IL of different regions fuel meat. The Al/(U+Mo) ratio had insignificant variation over the IL thickness of a selected particle. The ratio increases close to the matrix interaction boundary; and decreases near the fuel particle.

In the IL of mini-rods with 2% and 5% Si content in the matrix, the $(Al+Si)/(U+Mo)$ ratio depends on the Si content in the layer. In case of wide interaction layer, there is no Si. It concentrates on the Al interaction boundary. In this layer, the $(Al+Si)/(U+Mo)$ ratio ranges from 5.2 to 5.9. If there is more than 7at.% of Si in the IL, this ratio decreases to 4.7. Fuel particles with more than 7at.% Si content in the IL have an 1-2 μm wide IL (13% of Si in the matrix). IL without Si up to 10-15 μm wide may appear around other particles.

3.2. XRD

Samples for X-raying were mini-rods longitudinal sections of two types with U-7.5 %Mo (γ) and U-7.5 %Mo ($\alpha+\gamma$) type fuel. The examination was done by means of DARD-5 diffractometer using the stepped scanning technique (step 2θ 0.02 deg., exposure 2s). X-ray wave length corresponds to that of copper $\kappa\alpha$; graphite was used as a monochromator. The X-ray pattern of the unirradiated sample of U-7.5 %Mo (γ) type fuel and irradiated up to ~45% U-235 burn-up one are shown in Fig.3 and Fig.4, correspondingly. The obtained X-ray patterns were indexed as diffraction of two phases – Al and γ -U. The calculated parameters of unit cells made up as follows:

unirradiated sample: γ -U $a = 0.34186 \pm 0.00024$ nm, Al - $a = 0.40502 \pm 0.00005$ nm;

irradiated sample: γ -U $a = 0.34313 \pm 0.00016$ nm, Al - $a = 0.40506 \pm 0.00005$ nm.

It is evident from the obtained results, that the parameter of γ -U unit cell increased by 0.37% after irradiation. The parameter of Al unit cell remained unchanged.

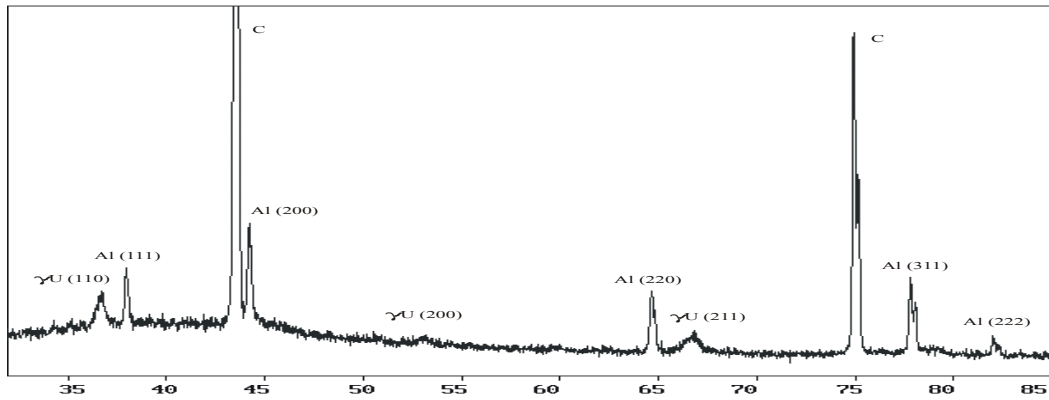


Fig.3. X-ray pattern of unirradiated sample U-7.5 %Mo (γ), C – diamond position.

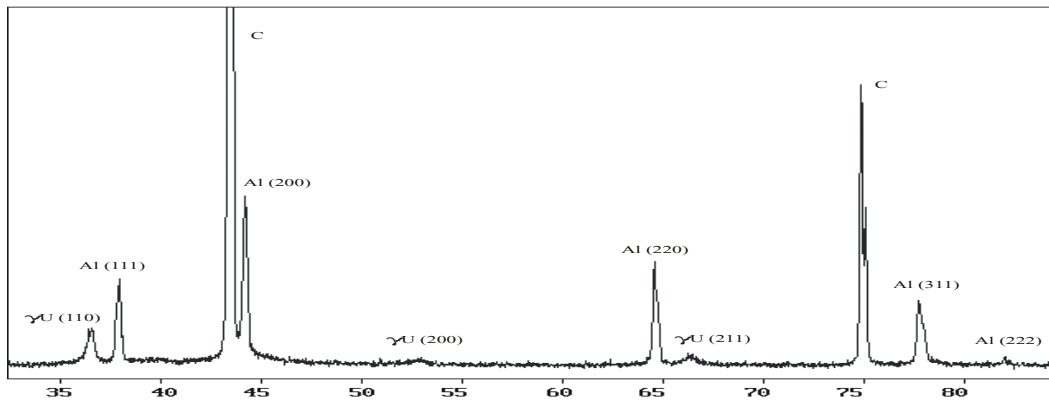


Fig.4. X-ray pattern of sample U-7.5 %Mo (γ) with ~45% U-235 burn-up.

X-ray patterns of the unirradiated and irradiated up to burnup of ~67% U-7.5 %Mo ($\alpha+\gamma$) fuel samples are shown in Fig.5 and Fig.6, correspondingly. The phase analysis of the X-ray pattern of the unirradiated sample showed three phases: α -U (orthorhombic lattice), γ -U, Al.

Calculated parameters of unit cells in the unirradiated sample made up:

α -U - $a = 0.28561 \pm 0.00012$ nm, $b = 0.58558 \pm 0.00037$ nm, $c = 0.49700 \pm 0.00021$ nm,

γ -U - $a = 0.34141 \pm 0.00040$ nm;

Al - $a = 0.40496 \pm 0.00002$ nm.

The X-ray phase analysis of the sample irradiated up to burnup of ~67% showed the presence of two phases: γ -U, Al.

Calculated parameters of unit cells in the irradiated sample made up:

γ -U - $a = 0.34273 \pm 0.00007$ nm; Al - $a = 0.40496 \pm 0.00002$ nm.

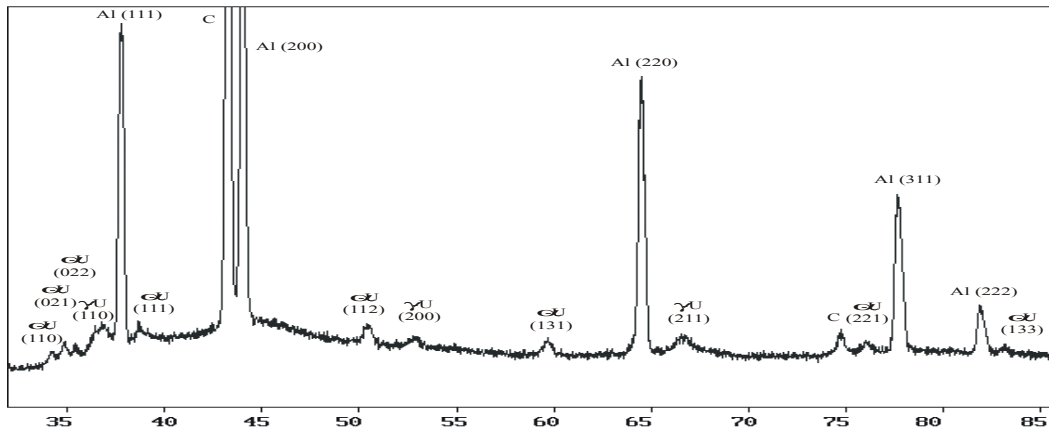


Fig.5. X-ray pattern of non-irradiated sample U-7.5 %Mo (α + γ).

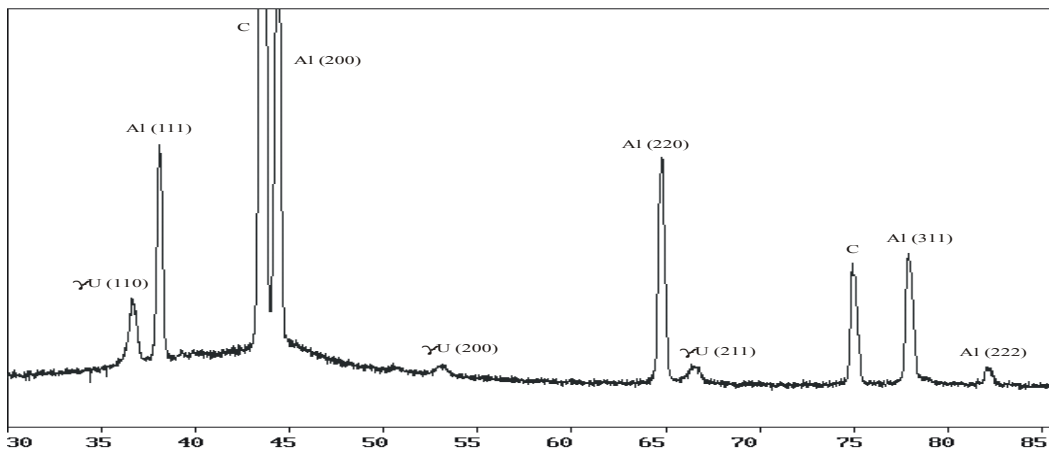


Fig.6. X-ray pattern of sample U-7.5 %Mo (α + γ) with burn-up ~ 67 % .

The obtained results show that irradiation resulted in disappearance of α -U phase and 0.39% increase in γ -U unit cell parameter. Al unit cell parameter did not change. Furthermore, it is worth considering the fact that no any other crystal phases were found in the irradiated samples except for Al and U.

Figure 7 presents the X-ray pattern of the sample U-9.4%Mo (γ) with burn-up ~ 85 %. As in the previous cases, the presented diffraction lines correspond to the structures of γ -U and Al. Calculated parameters of unit cells made up:

γ -U - $a = 0,3417 \pm 0,0002$ nm, Al - $a = 0,40499 \pm 0,00002$ nm.

Considerable width of diffraction lines γ -U (0,91 grad for line 310 and 1,9 grad for line 321) should be noted that is evident of a significant distortion of the crystalline structure.

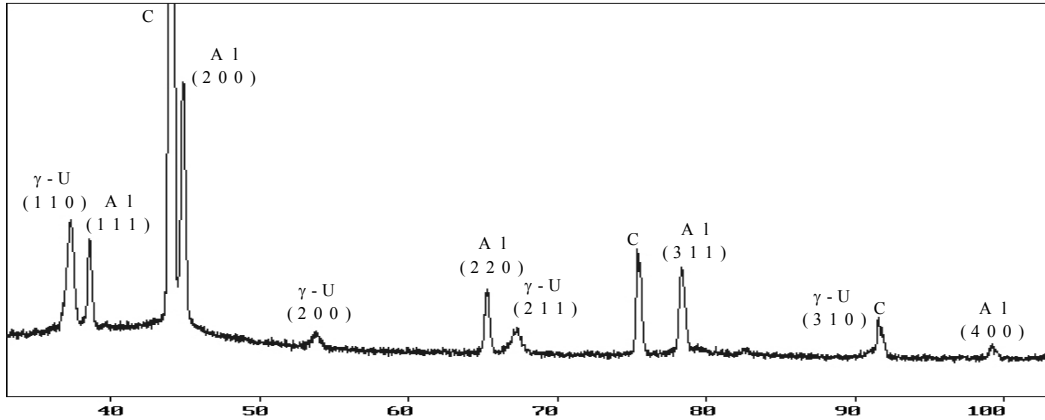


Fig.7. X-ray pattern of sample OM-9,4(γ) with burn-up \sim 85 %

Decrease of the Al lines intensity as compared to the previous X-ray patterns is evident of the Al content reduction in the fuel meat. The Al phase content reduction results from the formation of wide interaction layers. At the same time, a new phase formation was not found that is indirectly evident of the amorphous structure of the IL.

3.3. Generation of porosity in the U-9.4%Mo particles under irradiation.

The location of fission gas pores appeared in the U-Mo particles in the irradiated mini-rods was observed by SEM. To define exactly the pores location, mini-rods fractures were prepared. To produce a brittle fracture of fuel particles, the mini-rods were cooled with liquid nitrogen before fracturing. Figure 8 shows the fractures of pin-type mini-rods with 19.5% and 49.5% U-235 burnup.

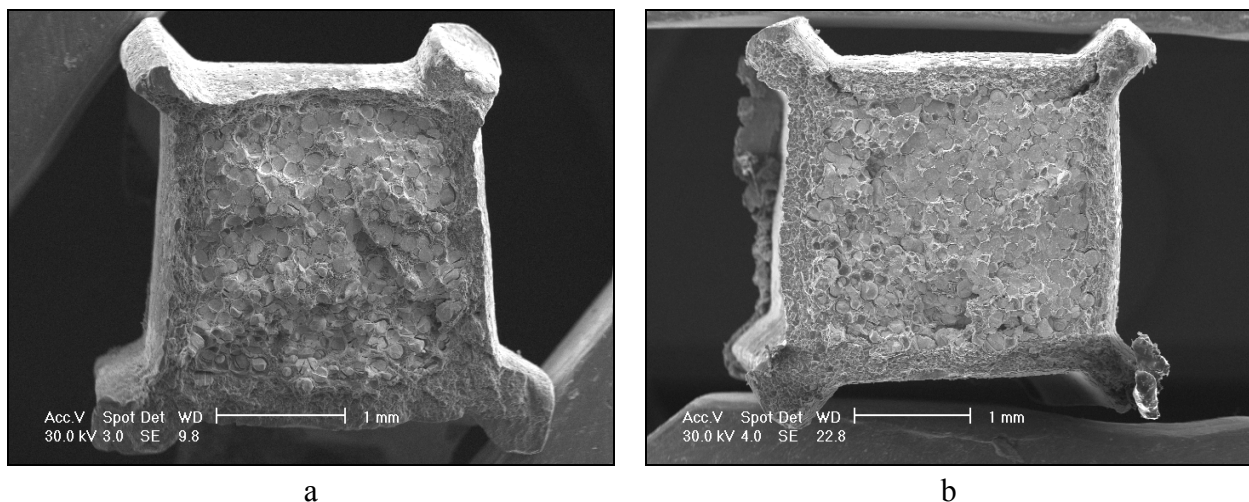


Fig. 8. Mini-rods fractures, U-9.4%Mo in Al matrix, (a) - 19.5% and (b) - 49.5% burn-ups.

The fractography shows that the pores appear on the grain boundaries at the beginning of irradiation (Fig.9). Based on these data, one may use polished samples to get further results (Fig.10).

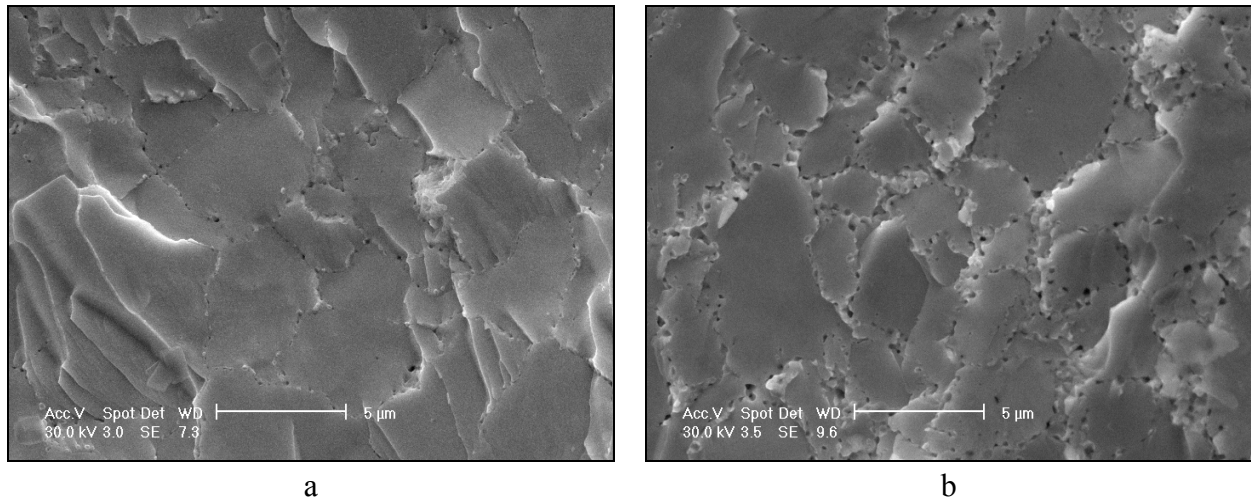


Fig. 9. FP gas bubbles in the U-9.4%Mo: (a) - 19.5% and (b) - 49.5% burnups.

It can be clearly seen on the polished samples that pores form the chains at the grain boundaries. At a burnup of 60%, the pore size at the grain boundaries increases up to $\sim(0.6-0.7) \mu\text{m}$. The grain boundaries become wider and pores are settled in several rows. The pores at the grain boundaries become larger at a U-235 burnup of 85%. Their maximal diameter achieves $\sim(1.0-1.3) \mu\text{m}$. A large amount of the secondary phase precipitates of submicron size are observed in the grain bodies. Pores appear in this phase. The identification of this phase by EPMA is rather complicated because of its small size. This evolution of the U-Mo particles structure is typical for all mini-rod fuel compositions concerned in this paper.

Similar structural changes are observed in the U-Mo particles of the full-size fuel rods (fig.11). Comparison of the microstructure of the fuel particles of these fuel rods with that of the U-Mo alloy particles of mini-rods shows the same nature of the porosity evolution in the full-size fuel rods and mini-rods.

Despite a significant increase in the U-Mo alloy porosity at a burnup of $\sim 85\%$, no large gas-filled bubbles are observed as well as no pore coagulation and pore chains. The pore diameter in the U-Mo alloy does not exceed $\sim 1.5 \mu\text{m}$. The typical pattern of pore size distribution in U-Mo fuel with the burnup of U 235 $\sim 60\%$ and $\sim 85\%$ is given in fig.12. Minimum pore size used to assess pores volume fraction made 50 nanometers.

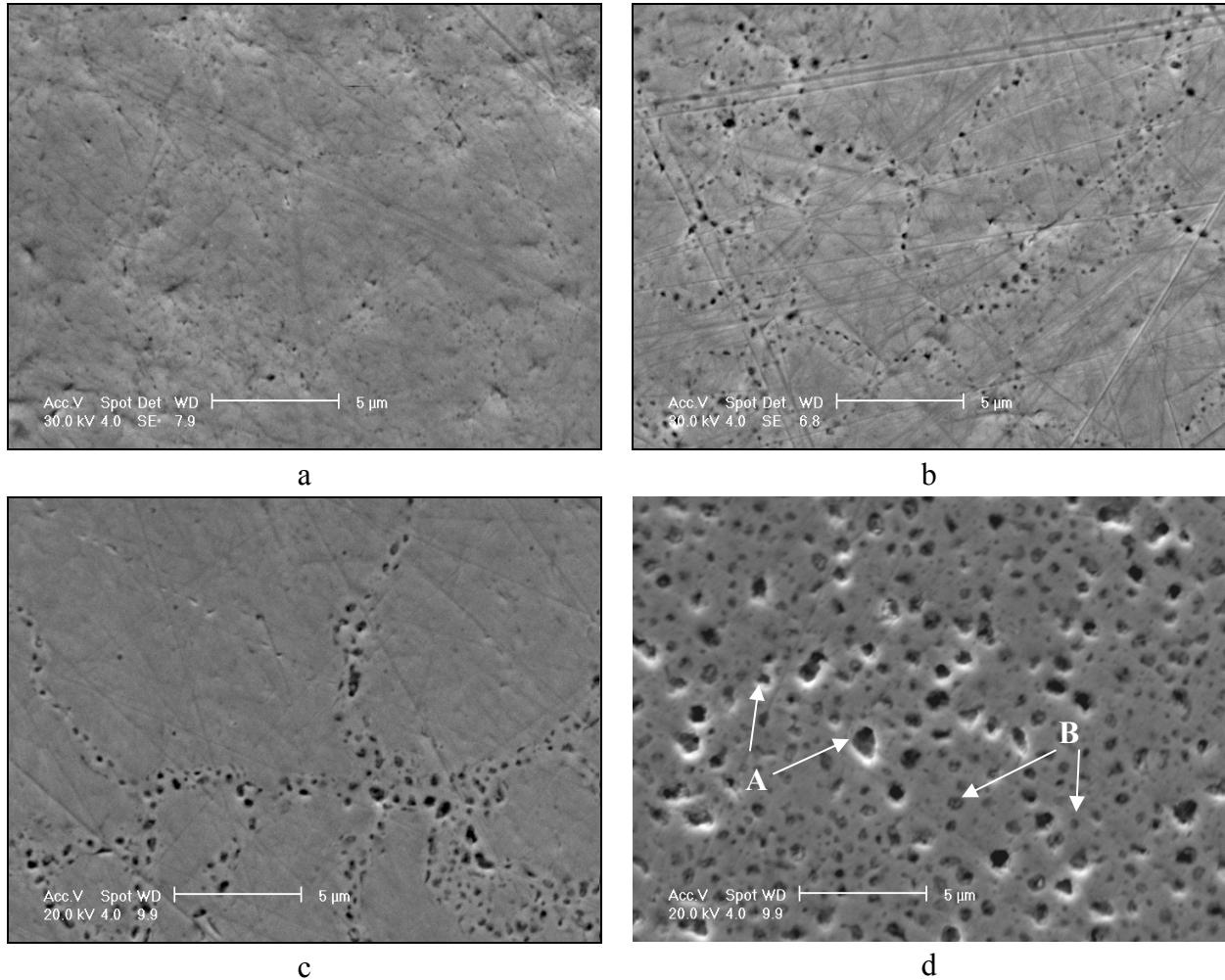


Fig. 10. Microstructure of the U-9.4%Mo particles in Al matrix at burnup of: (a) - 19.5%, (b) - 49.5%, (c) -58.8% and (d) - 85% (Arrows designated by letter A show the pores, arrows designated by letter B show the secondary phase precipitates).

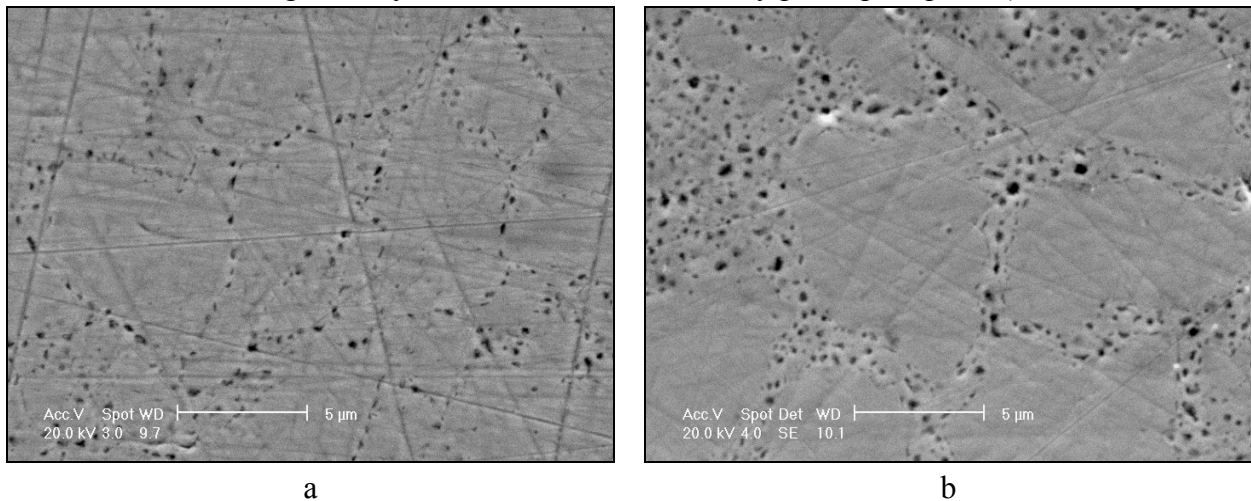


Figure 11. U-Mo alloy microstructure. Porosity distribution in the alloy: a – fuel rod from the FA with an average burnup of ~40 %, b – fuel rod from the FA with an average burnup of ~50 %

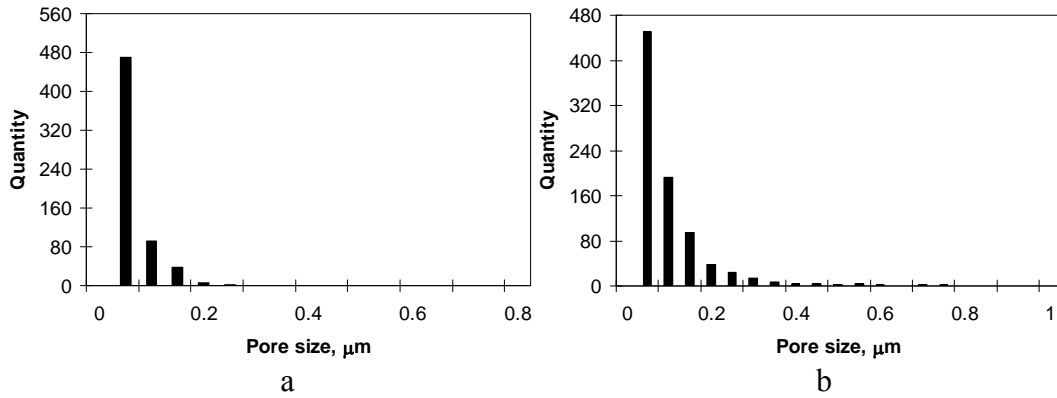


Fig.12. Pore size distribution in U-9.4Mo fuel: (a) - burn up of U 235 ~ 60%; (b) - burn up of U 235 ~ 85%.

Tab. 3 presents the results of the quantitative evaluation of the pores volume fraction (porosity).

Tab 3: Results of the quantitative evaluation of the porosity in ~ (100–140) μm U-Mo fuel granules

Fuel	Burnup,%	Fission density, 10^{21}cm^{-3}	Max fission rate, $10^{14}\text{cm}^{-3}\text{s}^{-1}$	IL thickness, μm	Porosity, %
Si<0.4%, 4 g U/cm ³	0	0	0	0	0,02
Si<0.4%, 4 g U/cm ³	~22	~1.5	~1.0	~2	1.18
Si<0.4%, 4 g U/cm ³	~53	~3.6	~1.0	~(3-5)	3.05
Si<0.4%, 4 g U/cm ³	~68	~4.5	~1.0	~(5-7)	12.44
Si<0.4%, 6 g U/cm ³	0	-	-	0	0,02
Si<0.4%, 6 g U/cm ³	~50	~3.4	~1.0	~(4-6)	3.1
Si<0.4%, 6 g U/cm ³	~65	~4.3	~1.0	~(6-8)	13.5
Si<0.4%, 6 g U/cm ³	~60	~4.1	~3.2	~ (25-30)	3,6
A1+2%Si, 6 g U/cm ³	~65	~4.3	~3.2	~ (15-30)	4,1
A1+5%Si, 6 g U/cm ³	~60	~4.1	~3.2	~ (2-30)	4,1
A1+13%Si, 6 g U/cm ³	~60	~4.1	~3.2	~ (2- 15)	4,4
Si<0.4%, 6 g U/cm ³ , ZrN coating	~60	~4.1	~3.2	-	4,8
Si<0.4%, 6 g U/cm ³	~80	~5.4	~2.3	~ (25-30)	11,6
A1+2%Si, 6 g U/cm ³	~80	~5.4	~2.3	~ (2-20)	11,9
A1+5%Si, 6 g U/cm ³	~84	~5.9	~2.3	~ (2-20)	13,2
A1+13%Si, 6 g U/cm ³	~84	~5.9	~2.3	~ (1-10)	14,9
Si<0.4%, 6 g U/cm ³ , ZrN coating	~90	~6.2	~2.3	-	15,2

Si<0.4%, 6 g U/cm ³ , IRT-U № 19УИ 0012006	53.1	~4.0	~2.6	~(10-12)	1.9
Si<0.4%, 6 g U/cm ³ , IRT-U № 19УИ 0022006	36.6	~2.8	~1.9	~(5-7)	1.0
Si<0.4%, 6 g U/cm ³ , IRT-U № 19УИ 0022006	47.2	~3.6	~1.9	~(6-8)	2.1
Si<0.4%, 6 g U/cm ³ , IRT-U № 19УИ 0022006	54.8	~4.2	~1.9	~(7-9)	4.7

Based on the results presented in Tab 3, a conclusion can be made that the porosity of the U-Mo alloy does not depend greatly on the irradiation conditions and fuel composition of the examined mini-rods. Some differences in the porosity for different compositions correspond to the differences in the IL value. Probably, the larger the volume fraction of this layer, the more GFP diffuse into it due to the higher temperature inside U-Mo particles.

Larger porous up to 2.5 μ m in diameter appear at the boundaries of interacting particles (Fig13- a). No pores were revealed at the matrix - IL boundary at a burnup of ~85%. At this burnup fine porosity is observed in the IL close to the particle boundary, pores diameter is less than ~1.0 μ m (Fig13- b).

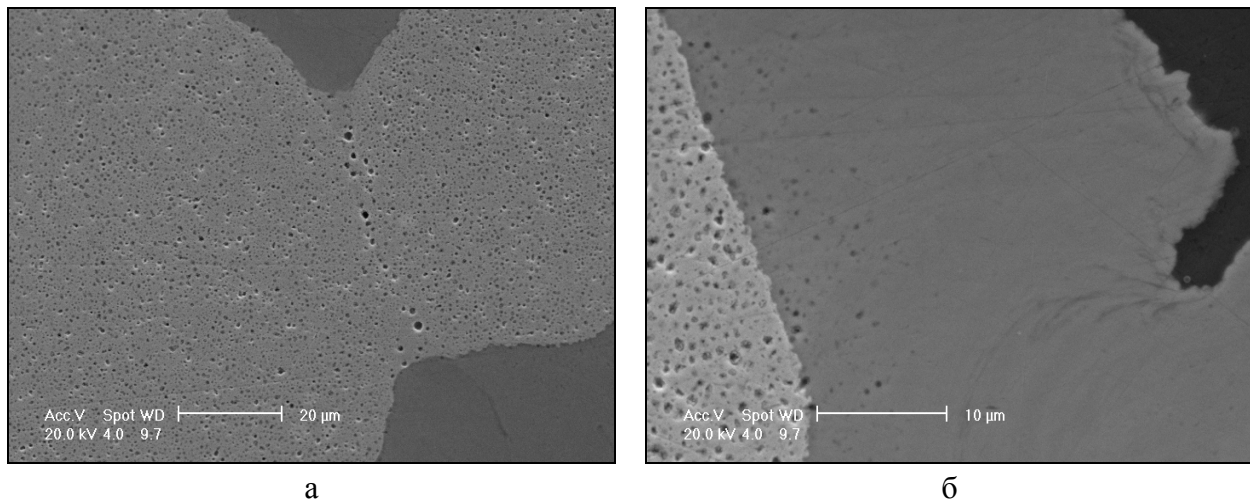
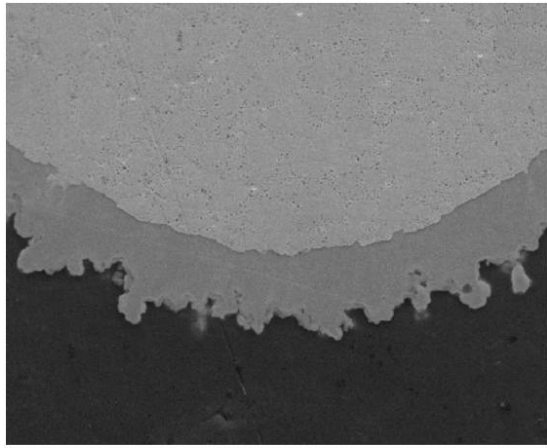
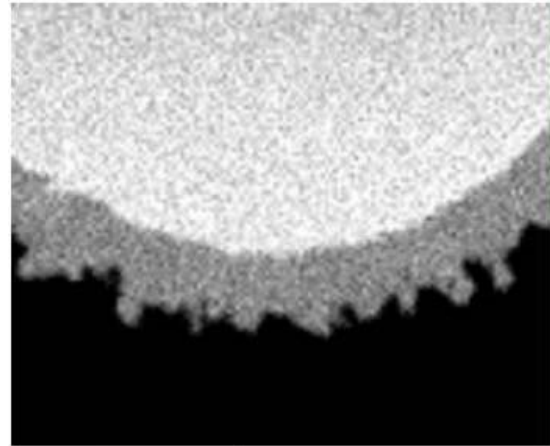


Fig. 13. Pores distribution U-9.4%Mo, 2% Si matrix, U-235 burnup ~ 80%:
(a) - at the boundary of the interacting particles; (b) - pores in the IL.

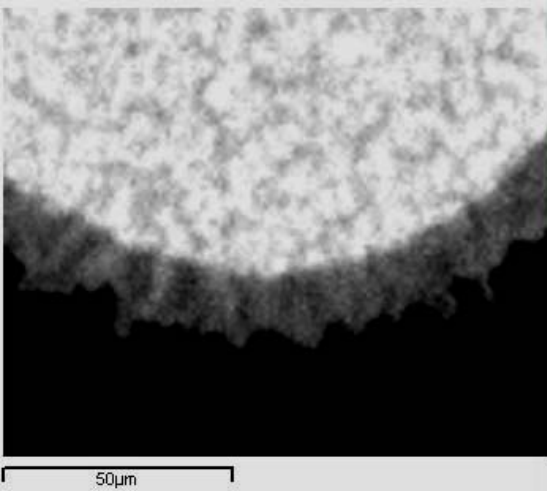
As the burnup of 65-70 % is achieved the porosity increases by ~ 3.2 times. Here, the redistribution of U FP is observed in the U-Mo alloy. Xenon and cesium are, mainly, in the solid solution at burnup of 60%. It can be proved by the Xe and Cs distribution maps (Fig.14). The grain boundaries are depleted in Xe and Cs. This is due the fact that these elements are concentrated in the micro-areas on the grain boundaries. Xenon forms gas-filled pores and cesium, probably, forms the secondary phase precipitates on the grain boundaries (e.g. CsI).



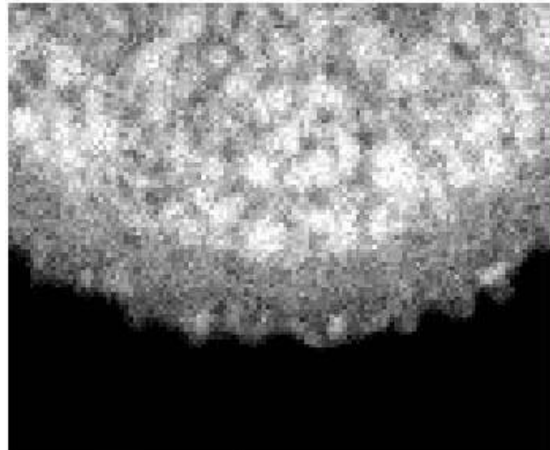
a



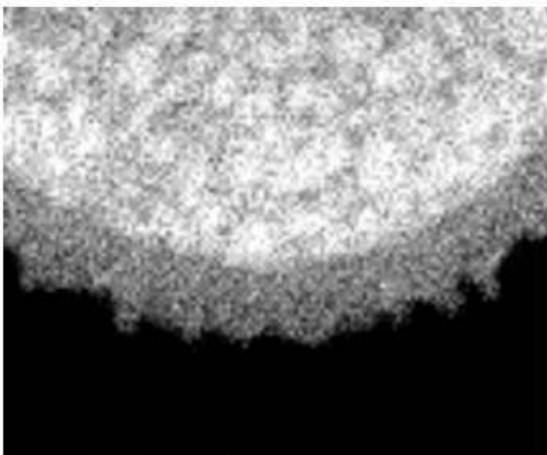
b



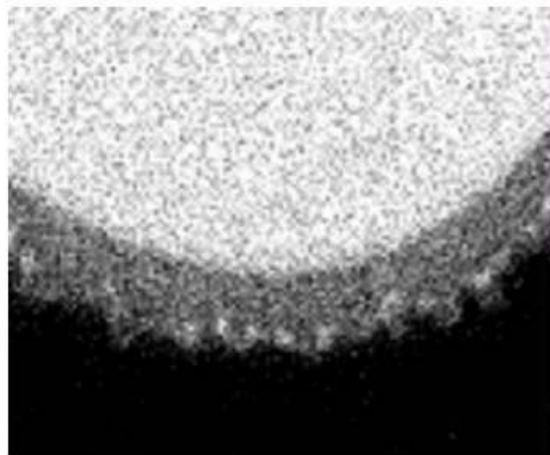
c



d



e



f

Fig. 14. (a) - fuel (5% Si , burnup ~60%) fragment and elements distribution maps:
(b) - U, (c) - Mo, (d) - Xe, (e) - Cs, (f) - Zr.

When preparing samples for examination (cutting and polishing), GFP volatilize out of the open porous while cesium and its compounds react with water and removed from the sample surface. The EPMA reflects only atoms of these elements remaining in the solid solution and Xe and Cs concentrated in the near-to-surface fine pores and secondary phase precipitates. Thus, the maximal concentration of these elements was registered by EPMA in the solid solution, secondary phase precipitates and pores located close to the sample surface.

As the 80% burnup is achieved, almost all Xe and Cs concentrate in the micro-areas forming a large amount of pores while the secondary phase precipitates appear both at the boundaries and inside the U-Mo alloy grains (Fig.15). The SEM photos show pores and secondary phase precipitates up to 1 μ m in size (Fig.10). The Zr distribution shows that it remains in the U-Mo alloy solid solution up to a U-235 burnup of ~ 85%.

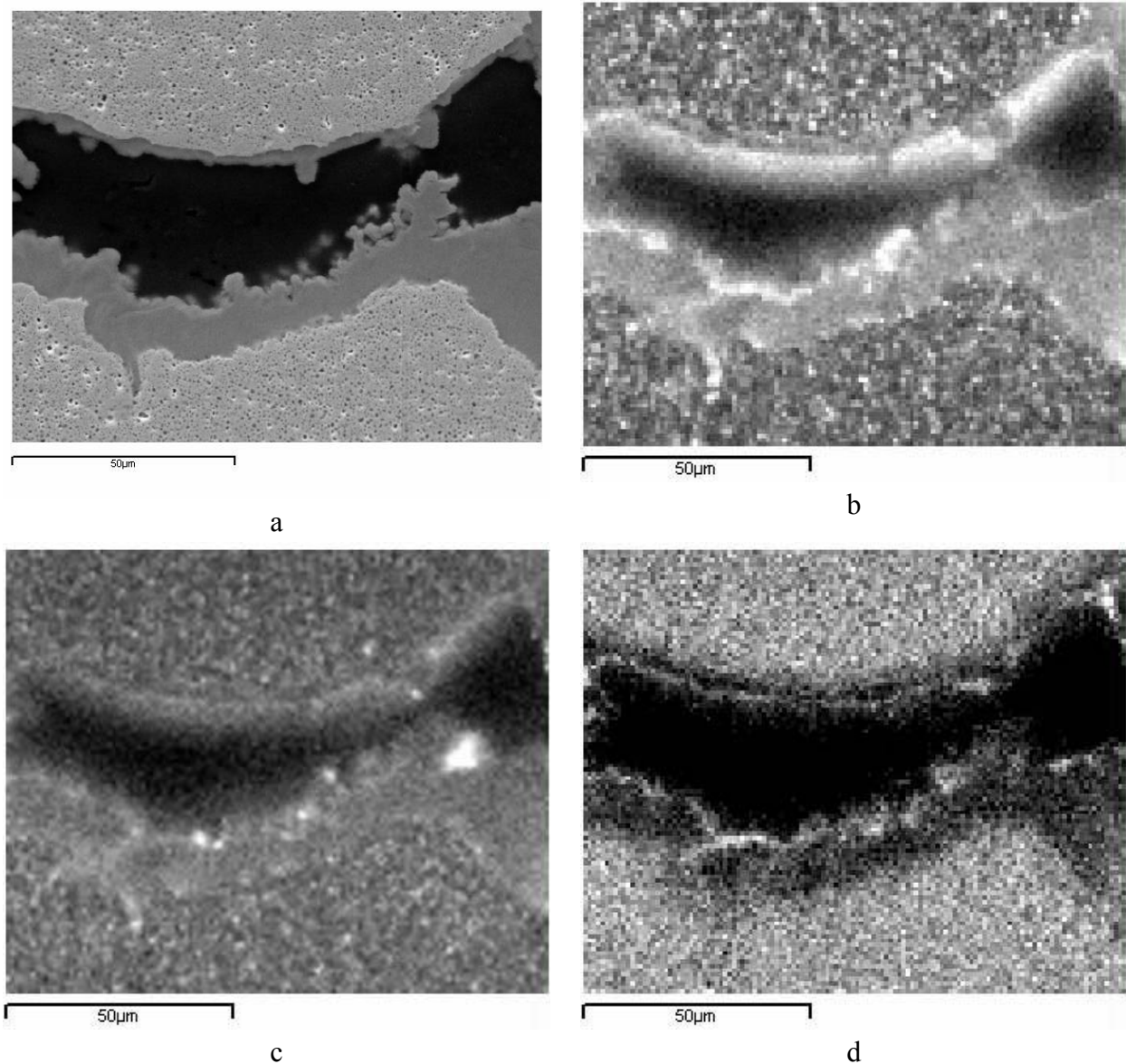


Fig. 15. (a) - fuel meat (5% Si, 80% burnup) fragment and elements distribution maps:
(b) – Xe, (c) – Cs, (d) – Zr.

Fig. 16 shows porosity of U-9,4%Mo fuel particles vs. fission density. At U-235 burnup of $\sim(65-70)$ % U-235 or $\sim(13-14)$ % of total U or a fission density of $\sim (4,3-4,5) 10^{21}\text{cm}^{-3}$ a critical concentration of fission products in the fuel particles that results in some fuel restructurization and intensive porosity formation is achieved. With the further burnup growth, the intensity of the porosity formation decreases sharply.

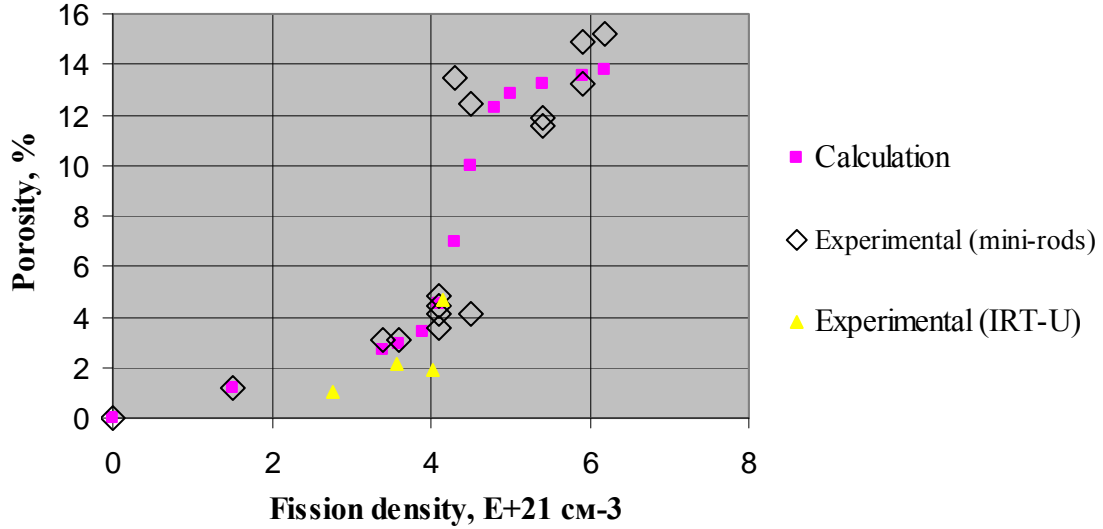


Fig. 16. Porous volume fraction vs. fission density

The porosity vs. fission density can be described as follows:

$$\Delta V/V = K_1(F^2 + (F/F_c)^{(2a+b)}) / (F + K_1/K_2 (F/F_c)^{2a}),$$

Where: F – fission density, $\times E^{-21}\text{cm}^{-3}$; $F_c=4.2$ – critical value of fission density; $K_1=3.58$, $K_2=12.5$, $a = 60$, $b = -0.7$ - constants.

It seems reasonable to perform additional investigations to clarify this dependence, including those at higher fission density values.

4. Discussion

The examination results of mini-rods with dispersed U-Mo/Al fuel confirms a well-known fact about a strong influence of the irradiation conditions on the intensity of the fuel-matrix interaction. The 1st batch, mini-rods with U density $\sim 4\text{g/cm}^3$ and $\sim 6\text{g/cm}^3$ were irradiated in the same irradiation rig; the fission rates in fuel particles were the same while thermal loads (heat rate and thermal flux from the surface) were in a direct proportion to the U density. One may definitely state that the temperature of the $\sim 4\text{gU/cm}^3$ fuel was $(10-15)^\circ\text{C}$ lower as compared to the $\sim 6\text{gU/cm}^3$ one, in which the temperature was $(85-105)^\circ\text{C}$. As a result of long-term irradiation, the thickness of the IL in the mini-rods with lower density tested at $10-15^\circ\text{C}$ lower temperature was $(1-2)\mu\text{m}$ less that made up 10-20% of the total layer thickness. To develop the calculation models describing the rate of the IL formation, we need the results of irradiation when the prescribed power and temperature were maintained for a long time. Unfortunately, when testing the 2nd batch, the thermal power changed cyclically in the wide range and a thick

(60-70 μm) oxide layer formed that made the determination and analysis of the temperature conditions rather complicated. Generally speaking, to provide experimental support of the calculation models, specific experiments separated parameters tests should be performed since when fuel is tested using standard RR cooling circuits, the inlet coolant temperature changes, as a rule, versus the reactor operating conditions while the power of experimental fuel rods changes both versus fuel burnup and reactor refueling.

The PIE of the pin-type mini-rods with dispersed U-Mo/Al fuel did not reveal any gas blistering in the fuel that was observed in the plate-like fuel rods [5] both in the Al IL and at the U-Mo particles boundaries under the irradiation conditions presented in the Tab 1. Perhaps, when testing the pin-type mini-rods with the above mentioned characteristics and irradiation conditions, the stresses and strain are not enough to fracture the fuel meat while this fact takes place during irradiation of plate-like rods up to a certain burnup.

The IL is uniform both regarding its structure and distribution of U and Al over the thickness (Fig.2). The atomic ratio Al/(U+Mo) in the matrix of pure Al is within the range of $\sim (7-9)$; this value is much higher than the data obtained in the experiments IRIS-1 $\sim (6-7)$, IRIS-2 $\sim (4,4-5,8)$ and FUTURE (3,3-4,7) [6, 7]. In the matrix with 2% and 5% Si contents the ratio between the number of atoms of (Al+Si)/(U+Mo) is $\sim (5-6)$ and these data agree with the results in ref. [8, 9]. Since Si suppresses the Al and U inter-diffusion, the lower (Al+Si)/(U+Mo) atomic ratio in the alloyed matrix as compared to the Al/(U+Mo) atomic ratio in the pure Al matrix has grounds. In the Al-U system there are three intermetallic compounds: UAl_2 , UAl_3 and UAl_4 . As one can see, the Al and U atomic ratio show none of these compounds in the IL. The X-raying of fuel with pure Al matrix irradiated up to the 45%, 65% and 85% U burnup showed that there were no any other crystalline phases except for Al and U. Numerous SEM and OM examinations did not reveal any phase precipitates in the IL. Probably, the IL is some kind of a non-stoichiometric amorphous alloy of Al and U. Another interesting fact is that at high burnups and thick diffusion layer ($\sim 20\mu\text{m}$) pores appear in the fission fragments free path $\sim 10\mu\text{m}$ wide U-Al layer (Fig.13b). Thus, the IL is not transparent for GFP and when a certain GFP concentration is achieved, gaseous porosity appears in the IL, the pores are larger near the fuel particle boundary.

The examination of the 1st batch [4] samples as well as the 2nd one and IRT-U FAs showed that at U-235 burnup of $\sim(65-70)\%$ or $(\sim 12-14)\%$ from the total U amount or at a fission density of $\sim 4.5 \times 10^{21} \text{cm}^{-3}$, the formation of gaseous porosity in the fuel particles became more intensive; the size and number of pores became higher at the U-Mo grain boundaries and pores grew in the grain. In addition, new phase precipitates appeared both at the boundaries and in the U-Mo grains. With further enhancement of burn up of U-235 from $\sim 70\%$ to ~ 90 the rate of pore formation abruptly declines. The XRD of samples irradiated up to burnups of $\sim 45\%$ and $\sim 67\%$ showed that the parameter of a γ -U unit cell increased by $\sim 0.37\%$ and $\sim 0.39\%$, respectively

Swelling of fuel particles could be divided into three components:

- 1) swelling caused by the increase of the U lattice parameter and increase of the unit cell volume by 1.16% at a burnup of $\sim 67\%$. The increase of the U crystalline structure parameter practically stops when a burnup of 45% is achieved;
- 2) solid swelling caused by solid fission fragments that are new phase precipitates at high burnups;
- 3) swelling due to gas pores formation having an evident nonlinear dependence on the burnup; moreover at $\sim 4.5 \times 10^{21} \text{cm}^{-3}$ fission density there is a kink region when the gas porosity formation process intensifies abruptly, then after the fuel restructuring the rate of transformation decreases abruptly.

An interesting fact was noticed at PIE fuel with Si alloyed matrix [2], the peripheral zone of some U-Mo particles was enriched with Si and in that layer porosity forming was essentially less than in U-Mo particle on the whole.

In our opinion to suppress the effect of an abrupt increase of the gas porosity at attaining a certain critical value of the fission density ternary U-Mo-Si systems could be perspective. At the same time the interaction between U-Mo-Si and Al-matrix can be suppressed and the effect of gas swelling can be reduced.

5. Conclusion

The IL of the U-Mo particles with the matrix in the pin-type mini-rods irradiated up to U-235 burnup of ~ 85% is uniform both regarding its structure and distribution of U and Al over the thickness. The EPMA showed that the Al/(U+Mo) atomic ratio in the pure Al matrix was in the range ~ (7-9). As for the 2% and 5% Si matrix, the (Al+Si)/(U+Mo) atomic ratio made up ~ (5-6). The X-raying of fuel with pure Al matrix irradiated up to U burnup of 45%, 67% and 85% showed no crystalline phases, except for U and Al ones.

At a U-235 burnup of ~(65-70)% or (~12-14)% from the total U amount or at a fission density of $\sim 4.5 \times 10^{21} \text{cm}^{-3}$, the formation of gaseous porosity in the fuel particles became more intensive; the size and number of pores became higher at the U-Mo grain boundaries and pores grew in the grain.

Swelling of fuel particles could be divided into three components:

- 1) swelling caused by the increase of the U lattice parameter and increase of the unit cell volume by 1.16% at a burnup of ~67%. The increase of the U crystalline structure parameter practically stops when a burnup of 45% is achieved;
- 2) solid swelling caused by solid fission fragments that are new phase precipitates at high burnups;
- 3) swelling due to gas pores formation having an evident nonlinear dependence on the burnup; moreover at $\sim 4.5 \times 10^{21} \text{cm}^{-3}$ fission density there is a kink region when the gas porosity formation process intensifies abruptly, then after the fuel restructuring the rate of porosity formation decreases abruptly.

The data on the structure of the fuel meat and porosity of the U-Mo alloy particles of the full-size fuel rods agree with the obtained behavior for mini-rods. Sharp increase of the U-Mo alloy porosity at a burnup within 40-60 % was observed in the fuel rods of the IRT-U FAs.

References

- [1] A.L. Izhutov, V.V. Alexandrov, A.Ye. Novosyolov et al., “The status of LEU U-Mo fuel investigation in the MIR reactor”, The 2009 International Meeting on Reduced Enrichment for Research and Test Reactors, November 1-5, 2009, Beijing, China.
- [2] A.L. Izhutov, V.V. Alexandrov, A.Ye. Novosyolov et al., “The main results of investigation of modified dispersion LEU U-Mo fuel tested in the MIR reactor”, The 2010 International Meeting on Reduced Enrichment for Research and Test Reactors, October 10-15, 2010, Lisbon, Portugal.
- [3] Yeon Soo Kim, G.L. Hofman, J. Rest, “Analysis of Fission Gas Bubbles and Microstructures of Irradiated U-Mo Fuel”, The 2009 International Meeting on Reduced Enrichment for Research and Test Reactors, November 1-5, 2009, Beijing, China.
- [4] A.L. Izhutov, V.V. Alexandrov, A.Ye. Novosyolov et al., “Results of PIE pin type LEU U-Mo fuel elements tested in the MIR reactor”, The 2006 International Meeting on Reduced Enrichment for Research and Test Reactors, Cape Town, Republic of South Africa, October 29-November 2, 2006.
- [5] G.L. Hofman, M.R. Finlay, Y.S. Kim, “Post-Irradiation Analysis of Low Enriched U-Mo/Al Dispersion Fuel Miniplate Tests, RERTR 4 and 5,” Proceedings of the 26th International Meeting on Reduced Enrichment for Research and Test Reactors, Vienna, Austria, Nov. 7–12, 2004.
- [6] Leenaers, A., S. Van den Berghe, E. Koonen, C. Jarousse, F. Huet, M. Troabas, M. Boyard, S. Guillot, L. Sannen, and M. Verwerft, 2004, “Post-irradiation Examination of Uranium-7 wt% M Molybdenum Atomized Dispersion Fuel,” *Journal of Nuclear Materials*, Vol. 335, pp. 39–47.
- [7] Ho Jin Ryu, Yeon Soo Kim, G.L. Hofman, D.D. Keiser. Characterization of the Interaction Products in U-Mo/Al Dispersion Fuel from In-pile and Out-of-pile Tests. 2006 RERTR International Meeting, Cape Town, Republic of South Africa, October 29 – November 2, 2006.
- [8] Gan, J., D. D. Keiser, D. M. Wachs, A. B. Robinson, B. D. Miller, T. R. and Allen, 2009, TEM Characterization of Irradiated RERTR Dispersion Fuel, RRFM 2009, March 23–25, 2009, Vienna, Austria.
- [9] Interaction Layer Characteristics in U-xMo Dispersion/Monolithic Fuels. INL/EXT-10-17972, Revision1.